# DISCHARGE OF FIRE SUPPRESSION AGENTS FROM A PRESSURIZED VESSEL: A MATHEMATICAL MODEL AND ITS APPLICATION TO EXPERIMENTAL DESIGN*

Leonard Y. Cooper
Fire Modeling Group
Building and Fire Research Laboratory
National Institute of Standards and Technology
Gaithersburg, MD 20899
(301) 975-6880

Presented at the

Halon Alternatives Technical Working Conference 1993

May 11 - 13, 1993
Albuquerque, New Mexico

*Sponsored by the U.S. Air Force Wright Patterson Laboratory

# DISCHARGE OF FIRE SUPPRESSION AGENTS FROM A PRESSURIZED VESSEL: A MATHEMATICAL MODEL AND ITS APPLICATION TO EXPERIMENTAL DESIGN

Leonard Y. Cooper
Building and Fire Research Laboratory
National Institute of Standards and Technology

## ABSTRACT

A mathematical model and associated computer program is developed to simulate the discharge of fire extinguishment agents from $N_2$-pressurized vessels. The model has three applications. First, to establish an experimental design and procedure which closely simulates discharge of a field-deployed vessel; second, to evaluate the discharge characteristics of a wide range of alternative-agent/pressure-vessel configurations, thereby extending the slow and relatively costly experimental method of making such evaluations; and finally, to predict vessel exit flow conditions to be used to solve the problem of agent dispersal outside of the discharge vessel. The model is used in example calculations which address the first of these applications.

The field-deployed system, which forms the basis of the example calculations, involves a half-liter cylindrical discharge vessel with a circular discharge nozzle/orifice of diameter 0.019m. The vessel is half-filled with liquid Freon 22 and is pressurized with $N_2$ to $41.37 \times 10^5$Pa (600psi). Vessel discharge is initiated by actuation of an explosive cap over the nozzle/orifice.

The simulating experimental configuration involves a modified field-deployed system. A diaphragm with nominal $41.37 \times 10^5$Pa (600psi) rupture pressure [actual values between $37.92 \times 10^5$Pa (550psi) and $44.82 \times 10^5$Pa (650psi)] replaces the explosive cap. The system is equipped with a high-pressure $N_2$ holding tank connected to the discharge vessel *via* an orifice. An experimental run begins with the onset of through-orifice $N_2$ flow from the holding tank. The vessel is pressurized to the point of diaphragm rupture and this is immediately followed by vessel discharge.

The model is used to simulate discharge of the field-deployed system and pressurization/discharge of the experimental system. Simulations of the experimental system involve holding tank volumes of $2.5 \times 10^{-3}$m$^3$ or $2.5 \times 10^{-5}$m$^3$; orifice diameters of 0.005m, 0.001m, or 0.0005m; and initial vessel pressures of $9.38 \times 10^5$Pa (136psi) (the saturation pressure of Freon 22 at 294K) and $34.47 \times 10^5$Pa (500psi).

From the calculations it was determined that the $2.5 \times 10^{-3}$m$^3$ holding tank with the 0.0005m orifice could be used to simulate accurately the discharge of the field-deployed system and that it is reasonable to expect that this experimental design would give good simulations even when extended to a range of parameters and agent materials well beyond the scope of the present calculations. Calculations also indicated that use of the $2.5 \times 10^{-5}$m$^3$ holding tank and/or the 0.005m orifice would not be consistent with an acceptable experimental design.

## THE PROBLEM AND THE OBJECTIVE

This work formulates a mathematical model to simulate the discharge of Halon and Halon-alternative fire extinguishment agents from $N_2$-pressurized vessels. The objective is to develop a mathematical model which simulates agent-discharge experiments under way at the Building and Fire Research Laboratory (BFRL) of the National Institute of Standards and Technology (NIST). The experiments are part of a program to support advances in fire safety in aircraft of the US Air Force.

The model is expected to have three applications. First, it will be used to establish an experimental design and procedure which closely simulates discharge of field-deployed vessels while allowing for acquisition of data, including high speed photography, to characterize adequately the discharge process. Second, the model will be used to evaluate the discharge characteristics of a wide range of alternative-agent/pressure-vessel configurations, thereby extending the slow and relatively costly experimental method of making such evaluations. Finally, it will be used to determine the discharge vessel exit-flow conditions for use in the simulation of agent dispersal outside of the vessel. After presenting the mathematical model, this work will include example calculations which address the first of these applications. The analysis is based on the experimental arrangement depicted in Figure 1.

## THE EXPERIMENT AND THE MODEL ASSUMPTIONS

### The Experimental Arrangement

Refer to Figure 1. This represents the arrangement associated with discharge experiments being considered at NIST. The Figure 1 arrangement can also be used to describe the phenomena of discharge from vessels under field conditions.

The experimental arrangement involves a right cylinder discharge vessel at pressure $P_{DV}$, which would contain $N_2$-pressurized test agent, and a holding tank filled with mass $M_{HT,N2}$ of $N_2$ at pressure $P_{HT}$. The discharge vessel is of height $Z_{DV}$ and cross-sectional area $A_{DV}$. The volume of the holding tank is $V_{HT}$.

The holding tank is connected *via* an orifice of area $A_O$ to the discharge vessel. It is assumed that the flow path through the orifice can be opened or closed with a relatively fast-acting solenoid valve. If the path is open it is assumed that $P_{HT} \geq P_{DV}$, i.e., the flow is always from the holding tank to the discharge vessel. In the case of a field-deployed system there is no holding tank and $A_O$ is zero.

At the bottom of the vessel is a short-nozzle/orifice-type opening of area $A_N$. The agent will be discharged through this to the outside ambient environment which is at pressure $P_{AMB} < P_{DV}$. The discharge flow path is originally closed off by a cap or diaphragm. When the cap is removed, the test agent liquid is driven out of the discharge vessel by virtue of the cross-nozzle/orifice pressure difference.

**The Procedure Prior to An Experimental Run or a Field-Deployed Discharge**

The orifice and nozzle/orifice flow paths are closed and the discharge vessel is evacuated. The vessel is then filled completely with a known mass of test agent. There will be a volume of liquid agent below and a volume of gaseous agent above and the pressure will be $P_{SAT}$, the saturation pressure at the agent temperature. The vessel is then pressurized with $N_2$. This flows into the vessel from the holding tank or from some other relatively high-pressure $N_2$ source. In general, the upper gas volume is now a two-component mixture of $N_2$ and test agent gas. Although some $N_2$ may be dissolved in the liquid volume, it is assumed that the amount is always so small that throughout subsequent sequential (additional-)pressurization and discharge processes to be studied here the properties of the liquid in the discharge vessel are well approximated by the liquid properties of the pure test agent.

Now consider the system at the time, $t = 0$, when an experimental run or a field-deployed discharge is initiated. The liquid/gas interface is a distance $Z_1$ above the bottom of the vessel. The mass of liquid in the vessel is $M_{DV,AL}$ (the subscript refers to that portion of Discharge Vessel test Agent in the Liquid state) and, throughout the experimental run or field-deployed discharge, the temperature and density of the liquid that remains in the vessel will be assumed to maintain their respective initial values, $T_{AL}$ and $\rho_{AL} = \rho_{SAT}(T_{AL})$. As indicated, $\rho_{AL}$ is estimated to be the density of saturated test agent liquid at the saturation temperature $T_{AL}$. The gas mixture is at an assumed uniform initial temperature $T_{DV,1}$ and the initial masses of gaseous test agent and $N_2$ in the discharge vessel are $M_{DV,AG}$ and $M_{DV,N2,1}$, respectively. Note that the pre-pressurization process, prior to $t = 0$, may have been so rapid that the liquid and gas are not in thermal equilibrium with each other. For this reason, $T_{DV,1}$ is not necessarily identical to $T_{AL}$. The discharge vessel and the holding tank are at the uniform pressures $P_{DV,1}$ and $P_{HT,1}$, respectively.

**During an Experimental Run or Field-Deployed Discharge**

During discharge of a Figure 1-type system, the flow path through the orifice is either open or closed at $t = 0^+$. When the orifice is closed the discharge will simulate discharge of a field-deployed system which does not involve a holding tank. When the orifice is open the discharge will simulate discharge of the experimental system where additional $N_2$ pressurization during the discharge is provided by the holding tank. The flow path through the nozzle/orifice at the exit of the discharge vessel is either opened at $t = 0^+$ (as in the field-deployed system, which uses an explosive cap to initiate discharge from an equilibrium state at the specified $P_{DV,1}$) or else it opens if and when $P_{DV}$ rises to some specified diaphragm rupture/burst pressure, $P_{BURST} < P_{HT,1}$ (as in the experimental system). The time when this latter flow path is opened is designated as $t_{BURST}$.

**Further Assumptions**

For times and conditions of interest it is assumed that as long as liquid remains in the vessel $P_{DV} > P_{SAT}(T_{AL})$ and there is no possibility of flashing (i.e., spontaneous change from a thermodynamically unstable liquid state to an equilibrium, two-phase, liquid/gas state) in the liquid volume. Future work will address the problem of removing this latter constraint from the analysis. It is assumed that any $N_2$ dissolved in the liquid that may come out of solution during the discharge process is negligible.

The purpose of this work is to mathematically model the state of the system at any $t > 0$ up to $t_D$, where $t_D$ is the smaller of 1) the time when the discharge vessel is emptied of test-agent liquid, and 2) the time when $P_{DV}$ is reduced to $P_{SAT}(T_{AL})$.

For experimental systems of interest here $t_{BURST}$ is expected to be of the order of 10s and the time interval of the discharge process, $(t_D - t_{BURST})$, of the order of $10^{-2}$s. Prior to $t_D$ there is no gas mixture discharge from the vessel. The mass of gaseous agent in the vessel therefore remains constant at its initial value $M_{DV,AG}$.

In view of the relatively short times of interest it is assumed that during an experimental run or field-deployed discharge there is no heat or mass transfer across the liquid/gas interface. It is also assumed that there is no heat or mass transfer across the interface that contains the nitrogen and gaseous test agent in the combined holding-tank/discharge-vessel system, e.g., there is negligible heat transfer to the walls of the vessel and holding tank. This is the basis of the assumption that both $M_{DV,AG}$ and the total mass of $N_2$ in the combined system, designated as $M_{N2}$, are constant for all t, $0 < t < t_D$. $M_{N2}$ is determined from the initial conditions.

It is assumed that the gaseous test agent and the $N_2$ can be modeled as perfect gases with constant specific heats and gas constants, $C_{V,AG}$ $C_{P,AG}$, $R_{AG}$ and $C_{V,N2}$ $C_{P,N2}$, $R_{N2}$. The values of the specific heats, which depend on temperature, are taken to be those which correspond to $T_{DV,1}$.

## THE MODEL EQUATIONS

Together with specified parameters, the unknown time-dependent variables of the problem that define the state of system at an arbitrary time are: $P_{HT}$, $P_{DV}$, $M_{HT,N2}$, $M_{DV,N2}$, $M_{DV,AL}$, $T_{HT}$, $T_{DV}$, Z. Known/specified parameters would include: the initial values of these variables, $P_{HT,1}$, $P_{DV,1}$, $M_{HT,N2,1}$, $M_{DV,N2,1}$, $M_{DV,AL,1}$, $T_{HT,1}$, $T_{DV,1}$, and $Z_1$, respectively; the geometric parameters of the system, $A_O$, $A_N$, $A_{DV}$, $Z_{DV}$, $V_{HT}$; material properties of the test agent and of $N_2$; the constant value $M_{DV,AG}$; and nozzle/orifice discharge coefficients, to be introduced below. The equations governing the variables are:

Equations of State in the Holding Tank and in the Discharge Vessel and the Law of Partial Pressure in the Discharge Vessel

$$P_{HT} = (M_{HT,N2}/V_{HT})R_{N2}T_{HT} \tag{1}$$

$$P_{DV} = (M_{DV,AG}R_{AG} + M_{DV,N2}R_{N2})T_{DV}/[(Z_{DV} - Z)A_{DV}] \tag{2}$$

Conservation of Mass of $N_2$

$$M_{DV,N2} + M_{HT,N2} = \text{constant} = M_{N2} = M_{DV,N2,1} + M_{HT,N2,1} \tag{3}$$

Relation of Z to $M_{DV,AL}$

$$M_{DV,AL}/\rho_{AL} = A_{DV}Z \tag{4}$$

Reversible Adiabatic Expansion for $N_2$ in Holding Tank

$$P_{HT}/(M_{HT,N2})^{\gamma} = \text{constant} = P_{HT,1}/(M_{HT,N2,1})^{\gamma} \tag{5}$$

where $\gamma = C_{P,N2}/C_{V,N2} = R_{N2}/C_{V,N2} + 1$.

First Law of Thermodynamics for Entire Gas System

$$d[(M_{DV,AG}C_{V,AG} + M_{DV,N2}C_{V,N2})T_{DV} + M_{HT,N2}C_{V,N2}T_{HT}]/dt = P_{DV}A_{DV}dZ/dt \tag{6}$$

Flow Across the Orifice

$$dM_{HT,N2}/dt = \begin{cases} -C_{D,O}A_OP_{HT}\{[\gamma/(R_{N2}T_{HT})][2/(\gamma+1)]^{(\gamma+1)/(\gamma-1)}\}^{1/2} \\ \qquad \text{if } P_{HT}/P_{DV} \geq [(\gamma+1)/2]^{[\gamma/(\gamma-1)]} \text{ (i.e., choked flow)} \\ -C_{D,O}A_OP_{HT}(P_{DV}/P_{HT})^{1/\gamma}\{2\gamma[1 - (P_{DV}/P_{HT})^{(\gamma-1)/\gamma}]/[(\gamma-1)R_{N2}T_{HT}]\}^{1/2} \\ \qquad \text{if } P_{HT}/P_{DV} < [(\gamma+1)/2]^{[\gamma/(\gamma-1)]} \text{ (i.e., un-choked flow)} \end{cases} \tag{7}$$

where $C_{D,O}$ is the (compressible) flow coefficient for the orifice [1].

Flow Across the Nozzle/Orifice

$$dM_{DV,AL}/dt = \begin{cases} -C_{D,N}A_N[2\rho_{AL}(P_{DV} - P_{AMB})]^{1/2} & \text{if } P_{AMB} \geq P_{SP} \\ -C_{D,N}A_N[2\rho_{AL}(P_{DV} - P_{SP})]^{1/2} & \text{if } P_{AMB} < P_{SP} \end{cases} \quad (8)$$

Where $C_{D,N}$ is the flow coefficient for the nozzle/orifice and $P_{SP}$ is defined below. Assuming that $A_N/A_{DV} << 1$ in discharge vessels of interest here, in Eq. (8) the kinetic energy of the liquid upstream of the exit nozzle is neglected compared to the kinetic energy at, and immediately downstream of the nozzle.

**DEFINITION OF $P_{SP}$ AND COMMENTS ON EQ. (8)**

In Eq. (8) it is assumed that the liquid in the discharge vessel, at state $[T, P] = [T_{AL}, P_{DV} > P_{SAT}(T_{AL})]$, flows into and through the exit nozzle/orifice while moving along state paths of constant entropy. When the pressure of the liquid drops below its saturation pressure, the liquid is assumed to initiate its movement into the "vapor dome" as a metastable super-heated liquid.

For the generic pure material, the relevant P-V diagram which depicts the metastable states is sketched in Figure 2. This includes the region of metastable super-heated liquid states and the corresponding region of metastable subcooled vapor states. For a pure material the metastable liquid or vapor state can only be maintained where $(\partial P/\partial V)|_T < 0$ [2], i.e., only outside the locus of points, referred to as the spinoidal curve, where $(\partial P/\partial V)|_T = 0$. The spinoidal curve, sketched in Figure 2, passes through the critical state and has the superheated liquid region to its left and the subcooled vapor region to its right.

At any time during the discharge, $P_{SP}$ is defined as the particular pressure along the liquid-leg of the spinoidal curve of the test agent associated with the intersection of the spinoidal curve and the above-mentioned, instantaneous, constant-entropy paths. Since states along the spinoidal curve are states of unstable equilibrium where spontaneous nucleation will occur [2, 3], i.e., the constant-entropy metastable-state path of the liquid cannot be sustained at the state defined by the intersection point, it is conjectured that if $P_{SP} > P_{AMB}$ violent flashing of the liquid jet occurs where and when its pressure reaches $P_{SP}$. This would be upstream of a physically-unachievable, i.e., unstable, *vena contracta* at pressure $P_{AMB}$.

If $P_{AMB}$ is achieved prior to the $P_{SP}$ state then the top portion of Eq. (8) is used. For this circumstance the constant-entropy state of the possibly metastable superheated liquid at $P_{AMB}$ is a physically-admissible endpoint to the liquid-jet development process. The situation is consistent with the idea that: 1) the endpoint state coincides with the *vena contracta* of the jet; 2) the jet is convected for some distance downstream of this endpoint without substantial changes and at the *vena contracta* diameter; and 3) the jet eventually breaks apart due to fluid-dynamic and/or thermodynamic (flashing) instabilities. Note that the upper Eq. (8)-description of the nozzle flow rate of a superheated liquid as an incompressible, non-flashing fluid, is consistent with results reported in the literature, e.g., [4], for flow through sharp-edge orifices and short nozzles.

If $P_{SP}$ is achieved prior to $P_{AMB}$ then flashing of the metastable liquid will be initiated immediately downstream of the position in space where the intercept occurs. In the latter case the incompressible flow calculation methodology is still applicable at and upstream of the spinoidal-curve intercept point. This is indicated by the use of the bottom portion of Eq. (8).

The above discussion is illustrated with $CO_2$. For stable and metastable liquid $CO_2$, a sketch from [3] of constant-entropy paths in a P-T diagram is presented in Figure 3. In preparing this figure, the Peng-Robinson equation of state was used in [3] to describe the metastable liquid $CO_2$.

First assume that liquid $CO_2$ is in a Figure 1-type discharge vessel at $P_{DV} = 70x10^5$Pa and $T_{AL} = 288$K. In Figure 3 this initial state is seen to lie on the s = s2 constant-entropy line, which has no positive P intercept with the spinoidal curve. As the liquid $CO_2$ flows toward and then out of the vessel's nozzle/orifice its state is assumed to move downward along the s2 curve of Figure 3. As can be seen, the $P = P_{ATM} \approx 1x10^5$Pa intercept on this curve, corresponding to $T \approx 277$K, represents an achievable metastable liquid state for the material. This is the metastable liquid state that is predicted by the present model. It would be expected at, and for some distance downstream of, the jet's *vena contracta*.

Now assume that liquid $CO_2$ in a discharge vessel is at $P = P_{DV} = 60x10^5$Pa and $T = T_{AL} = 291$K. In Figure 3 this initial state is seen to lie on the s = s3 constant-entropy line, which intersects the spinoidal curve at approximately $P_{SP} = 10x10^5$Pa $>> P_{AMB}$. In this case, as the liquid $CO_2$ flows through and out of the vessel nozzle/orifice the model predicts that it will flash explosively when $P = P_{SP}$. This will occur upstream of the position at which a fluid jet *vena contracta* would otherwise occur; well within a distance of one nozzle/orifice diameter downstream of the vessel exit.

This nozzle/orifice flow model is consistent with a discharge process involving a smoothly time-varying $P_{DV}$, a constant $T_{AL}$, and an abrupt change in nozzle/orifice exit flow from a simple incompressible-fluid-jet type flow to an explosively flashing two-phase flow. This kind of discharge phenomenon was clearly observed during recent Freon 22 discharge experiments at NIST [5]. Note that the idea of using the condition of the existence of $P_{SP} > P_{AMB}$ as a criterion for violent flashing of liquids flowing through sharp-edged orifices or very short nozzle-like openings does not seem to have been proposed previously. Nor has it been validated quantitatively.

## REDUCED DIMENSIONLESS EQUATION SET - THE INITIAL VALUE PROBLEM

Eqs. (1) - (8) are made dimensionless by introducing a dimensionless time, $\tau$, dimensionless mass of $N_2$ and liquid agent in the discharge vessel, $x_2$ and $x_3$, respectively, and a combined variable, $x_1$.

$$x_1 = [(1 + \lambda_3 x_2)/(1 + \lambda_1 x_2)](P_{DV}/P_{DV,1})(Z_{DV}/Z_1 - x_3) + \lambda_2\lambda_4(1 - x_2)^{\gamma};$$

$$x_2 = M_{DV,N2}/M_{N2};\ x_3 = M_{DV,AL}/M_{DV,AL,1};\ \tau = tC_{D,N}A_N[2P_{DV,1}/(M_{DV,AL,1}A_{DV}Z_1)]^{1/2} \tag{9}$$

$$\lambda_1 = (M_{N2}/M_{DV,AG})(R_{N2}/R_{AG});\ \lambda_2 = (P_{HT,1}/P_{DV,1})/(M_{HT,N2,1}/M_{N2})^{\gamma};$$

$$\lambda_3 = \lambda_1(\gamma_{AG} - 1)/(\gamma - 1);\ \lambda_4 = [(\gamma_{AG} - 1)/(\gamma - 1)][V_{HT}/(Z_1A_{DV})]; \tag{10}$$

The initial values of the x's are functions of the various parameters of the particular problem of interest. The dimensionless initial value problem for an arbitrary Figure-1 configuration is

$$dx_i/d\tau = \sigma_i;\ \sigma_i = \sigma_i(x_1, x_2, x_3; \text{ parameters of the problem});\ x_i(0) \text{ specified, } i = 1, 2, \text{ or } 3 \tag{11}$$

The reader is referred to the Appendix of [6] for definitions of the $\sigma_i$ and for explicit equations to extract values of time-dependent dimensional variables from a solution of Eqs. (11).

## $N_2$ JET-DRIVEN MIXING IN THE DISCHARGE VESSEL - ESTIMATING THE RESULTING DISTURBANCE OF THE LIQUID/GAS INTERFACE

The above model assumes that throughout the pressurization and discharge process the agent gas and the $N_2$ in the discharge vessel are fully mixed and in a state of thermodynamic equilibrium. It is also assumed that there is no significant heat or mass transfer interactions at the gas/liquid interface, i.e., it is assumed that the interface is relatively quiescent.

In cases where there is no $N_2$ flow from the holding tank (e.g., the orifice is closed) the initial fully-mixed state of the gases will persist throughout de-pressurization, the gas volume will be relatively quiescent, and the assumption of negligible interface interactions is expected to hold. This is the case for actual field-deployed systems.

When there is $N_2$ flow from the holding tank, it is the $N_2$ jet from the orifice that will drive gas mixing in the discharge vessel. Refer to Figure 4. If jet velocities are too large, the liquid/gas interface disturbance of the jet can be violent enough to invalidate the quiescent interface assumption.

For the configuration of Figures 1 and 4, the significance of the effect of the $N_2$ jet impinging on the liquid surface can be determined from an estimate of the axial velocity of the orifice jet at the liquid/gas interface. Such an estimate is obtained here from the characteristics of an incompressible submerged jet (i.e., analogous to the $N_2$ orifice jet) in an unconfined space (analogous to the gas volume of the discharge vessel). The estimate is also useful for other orifice orientations.

Let the velocity on the jet axis a distance $Z_{JET} = Z_{DV} - Z$ from the orifice (i.e., at the elevation of the liquid/gas interface) be denoted by $U_{JET}$ and assume a uniform velocity, $U_O$, across the orifice opening

$$U_O = (dM_{DV,N2}/dt)/[A_O(M_{HT,N2}/V_{HT})] \quad (12)$$

From [7]

$$U_{JET}/U_O = 0.96/[0.066(2Z_{JET}/D_O)+0.29] \text{ for } 2Z_{JET}/D_O > 10. \quad (13)$$

When the time-dependent solution for $M_{DV,N2}$ is available, $U_{JET}$ can now be estimated from Eqs. (12) and (13) and the significance of the jetting phenomenon can be assessed.

## SOLVING THE MODEL EQUATIONS

A computer program was developed to solve the initial value problem of Eqs. (11) corresponding to an arbitrary choice of geometric parameters, material properties, and initial conditions, and to determine the value of $U_{JET}$ from Eqs. (12) and (13). The method of solution is based on the differential equation solver RKQC presented in [8]. The program was used in the example calculations to follow.

## EXAMPLE CALCULATIONS

### An Experimental Procedure to Simulate the Discharge of Field-Deployed Vessels

As mentioned in the introductory comments, the example calculations to be presented here focus on the establishment of an experimental design and procedure, where vessel discharge closely simulates the discharge of a field-deployed vessel while allowing for acquisition of data, including high speed photography, to characterize the discharge process.

Field-deployed systems use an explosive device to remove, "on demand," a cap covering the exit nozzle/orifice of a pre-pressurized discharge vessel. Thus, the deployed system is characterized by a Figure 1-type configuration with no holding tank component, i.e., with $A_O = 0$.

The nature of the experimental program at NIST precludes the use of an explosive cap device. The experimental procedure to be evaluated involves a vessel discharge process which is initiated, instead, by rupture of a nozzle/orifice diaphragm cap at a high cross-diaphragm pressure difference. The pressurization of the discharge vessel from $P_{DV,I}$ to the diaphragm burst pressure, $P_{BURST}$, is achieved with the use of the holding-tank/orifice-flow feature of Figure 1.

As discussed earlier, an experimental run involves sequential processes of vessel pressurization and discharge. Initially, the diaphragm cap prevents flow from the vessel to the outside environment. At $t = 0^+$ the orifice connecting the vessel and the holding tank is opened and pressurization of the vessel is initiated. At the instant the pressure in the vessel reaches the diaphragm burst pressure, the diaphragm ruptures. Nozzle/orifice flow and discharge of the vessel are then initiated. As mentioned earlier, the pressurization and discharge processes of interest here are expected to occur over time intervals of the order of 10s and $10^{-2}$s, respectively

Prior to any particular test run, $P_{BURST}$ is only known to an accuracy of approximately ten percent. Also, the high speed camera to be used to photograph the discharge process during the test procedure can record a total time interval no larger than the order of a few seconds, including an initial interval of approximately 1s required to bring the camera up to its operating speed.

### Criteria for Experimental Discharges to Closely Simulate Field-Deployed Discharges

One would hope to determine that an experimental discharge would closely simulate a field-deployed system discharge by obtaining good agreement between results of model simulations of the two processes. The basic criterion would be good reproduction of the predicted time-dependent values of $P_{DV}$ and $M_{DV,AL}$.

Since field-deployed discharges involve no addition of $N_2$ and no significant heat or mass transfer at the liquid/gas interface, an acceptable Figure 1-type experimental procedure should similarly involve discharges with no significant addition of $N_2$. In view of this, in addition to the above criterion two additional criteria must be satisfied if the experimental discharge is to simulate closely a field-deployed discharge: 1) the experiment must include a discharge process during which the total mass

of $N_2$ delivered from the holding vessel to the discharge vessel is small compared to the mass of $N_2$ in the discharge vessel immediately prior to the onset of discharge, i.e.,

$$\text{require } (M_{N2} - M_{N2,B})/M_{N2,B} << 1 \text{ for } t > t_{BURST} \tag{14}$$

where $M_{N2,B}$ is the mass of $N_2$ in the discharge vessel at $t_{BURST}$; and 2) the addition of $N_2$ during the entire pressurization/discharge sequence does not lead to gas flows in the discharge vessel gas (where velocities will be of the order of $U_{JET}$) which are so vigorous as to lead to significant heat or mass transfer at the liquid/gas interface. It is reasonable to expect that interface surface interactions will not be significant if $U_{JET}$ - dZ/dt never exceeds the order of a few m/s. Thus

$$\text{require } U_{JET} - dZ/dt < 5 \text{ to } 10\text{m/s for } t \geq 0 \tag{15}$$

**Model Input Parameters**

Sets of parameters representative of those a Figure-1-type experimental design are presented in Table 1. These are selected to simulate discharge of a field-deployed system with a $0.5x10^{-3}m^3$ discharge vessel half-filled with liquid $CHClF_2$ and pressurized with $N_2$ to $41.37x10^5$Pa (600psi). Parameters of the field-deployed system are included in the table.

| agent | Chlorodifluoromethane/$CHClF_2$ (Freon 22) | | | | | | |
|---|---|---|---|---|---|---|---|
| $T_{DV,1}$ = $T_{HT,1}$ = | 294K | | | | | | |
| $D_{DV}$ = | 0.05m | | | | | | |
| $V_{DV}$ = | $0.5x10^{-3}m^3$ | | | | | | |
| $M_{DV,AL,1}$= | $\rho_{AL}(V_{DV}/2)$ = 0.302kg | | | | | | |
| $D_N$ = | 0.01905m | | | | | | |
| $V_{HT}$ = | $2.5x10^{-3}$m3 (large holding tank) | | | | $2.5x10^{-5}$m3 (small holding tank) | | field simulation |
| $P_{HT,1}$ = | $51.71x10^5$Pa (750psi) | | | | $155.13x10^5$Pa (2250psi) | | - |
| $P_{DV,1}$ = | $34.47x10^5$Pa (500psi) (Figs. 12 and 13) | | $9.38x10^5$Pa (136psi) = $P_{SAT}(T_{DV,1})$ (Figs. 6 and 7) | | $34.47x10^5$Pa (500psi) | | 41.37x $10^5$Pa (600psi) |
| $P_{BURST}$ = | 37.92x $10^5$Pa (550psi) | 44.82x $10^5$Pa (650psi) | 37.92x $10^5$Pa (550psi) | 44.82x $10^5$Pa (650psi) | 37.92x $10^5$Pa (550psi) | 44.82x $10^5$Pa (650psi) | 41.37x $10^5$Pa (600psi) (Figs. 14 and 15) |
| $D_O$ = | 0.0005m, 0.001m, and 0.005m | 0.0005m, 0.001m, and 0.005m | 0.0005m (Figs. 8, 14 and 15), 0.001m, and 0.005m (Fig. 9) | 0.0005m (Figs. 10, 14, and 15), 0.001m, and 0.005m (Fig.11) | 0.0005m (Fig 16 and 17), 0.001m, and 0.005m (Figs. 21 and 22) | 0.0005m (Figs. 18, 19, and 20), 0.001m, and 0.005m (Figs. 23 and 24) | - |

**Table 1. Characteristics of simulated discharges - model input parameters**

The parameters sets of Table 1 define simulations of 18 different experimental systems and the single simulation of the field-deployed system. The parameters sets were used to define and solve the model's initial value problem. Solution results provide time-dependent histories of all model variables and the information necessary to determine whether or not the criteria of Eqs. (14) and (15) are satisfied during the simulation. Solution results will be presented and discussed below.

As indicated, the model simulations involve the agent $CHClF_2$. In solving Eqs. (11) and (12) the following thermodynamic properties were used for this and for $N_2$:

Properties of Chlorodifluoromethane/$CHClF_2$ (Freon 22) [9].

$$\text{Mol. Wt.} = 86.469\text{kg/(kg-mole)};\ \rho_{AL} = \rho_{SAT}(294\text{K}) = 1209\text{kg/m}^3;\ C_{P,AG} = C_{P,AG}(300\text{K}) = 57(10^3)\text{J/(kg-mole·K)}$$

$$P_{SAT} = 6895(T/R)^{-C}[F - (T/R)]^{E[F-(T/R)]/[F(T/R)]}10^{A - B/(T/R) + D(T/R)}\text{Pa} \tag{16}$$

$$A=29.35754453;\ B=3845.193;\ C=7.86103122;\ D=0.002190939044;\ E=305.826813;\ F=686.1$$

Properties of Nitrogen [10].

$$\text{Mol. Wt.} = 28.013\text{kg/(kg-mole)}$$

$$C_{P,N2} = [7.440 - 3.24(10^{-3})(T/K) + 6.400(10^{-6})(T/K)^2 - 2.790(10^{-9})(T/K)^3]4186\text{J/(kg-mole·K)} \tag{17}$$

where $T = T_{DV,1}$ was used to estimate (a constant value for) $C_{P,N2}$

**Other Assumptions on the Model Parameters**

The following completes the information used to fully define the model equations:

Flow coefficient for the nozzle/orifice (flow of test agent liquid from the discharge vessel to the outside environment).

$$C_{D,N} = 0.60 \tag{18}$$

Spinoidal pressure. Use of Eq. (8) and the $\sigma_1$ and $\sigma_3$ components of Eqs. (11) require values of $P_{SP}$ for isentropic paths from the time-dependent liquid states in the discharge vessel. For the present calculation it is assumed that throughout the discharge process $P_{SP} < P_{ATM} = 1.01\text{x}10^5\text{Pa}$ (14.7psi), i.e., spinoidal-curve type instabilities of the metastable exit liquid stream do not occur during the major portion of the discharge-process time interval. This assumption is consistent with previously mentioned Freon 22 discharge experiments at NIST [5]. However, as seen above in the discussion of $CO_2$, this assumption can not be expected to hold in general, and actual estimates of $P_{SP}$ will have to be included in more general applications of the mathematical model.

Flow coefficient for the orifice (flow of $N_2$ from the holding tank to the discharge vessel). $C_{D,O}$ for compressible flow through sharp-edged orifices as a function of cross-orifice pressure ratio, $P_{DV}/P_{HT}$ is provided in [11]. Data points for $C_{D,O}(P_{DV}/P_{HT})$ are plotted in Figure 5. In the present calculations, values of $C_{D,O}$ are estimated by linear interpolation between these data points.

Input value for $M_{DV,AG}$. To determine the constant mass of gaseous test agent in the discharge vessel it is assumed that the process of filling the vessel included a time when pure test agent filled the entire vessel with gas and liquid volumes in thermodynamic equilibrium with each other. The mass of gaseous agent at this time is taken to be $M_{DV,AG}$. In the present calculations it is assumed that at this time of equilibrium the agent temperature was 294K. This is the value taken above for the initial temperatures $T_{DV,1}$ and $T_{HT,1}$.

## RELATIVELY LOW-PRESSURE LARGE-VOLUME HOLDING TANK

This section will present results for the pressurization/discharge sequence using a relatively low-pressure large-volume holding tank. Note that experimental safety considerations motivate use of relatively low-pressures in the holding tank, especially when it is of relatively large volume.

$V_{HT}$ = $2.5x10^{-3}m^3$ is chosen to be ten times larger than the initial gas volume in the discharge vessel and $P_{HT,1}$ = $51.71x10^5$Pa (750psi) is chosen to be $6.89x10^5$Pa (100psi) greater than the maximum of the diaphragm burst pressure which can fall within the range $37.92x10^5$Pa < $P_{BURST}$ < $44.82x10^5$Pa (550psi < $P_{BURST}$ < 650psi).

The objective in the present choice of parameters is to provide for a pressurization process which is slow enough to minimize disturbances of the liquid/gas interface, i.e. satisfy Eq. (15), but fast enough to be able to bracket clearly the time of the subsequent discharge process to a known time interval of the order of 1s. The 1s time interval is required to guarantee timely triggering of and photographic data acquisition from a high-speed camera during the discharge process. As mentioned above, the latter is expected to occur over a time interval of the order of $10^{-2}$s.

The relatively large volume of the holding tank would allow the pressurization/discharge process to be initiated either: 1) from a relatively high-$P_{DV,1}$ state, somewhat below the minimum possible diaphragm burst pressure and with a relatively significant initial mass of $N_2$ in the discharge vessel; or 2) from a minimum-$P_{DV,1}$ state where there is no $N_2$ in the discharge vessel (i.e, the discharge vessel initially contains only pure test agent at the saturation pressure $P_{DV,1}$ = $P_{SAT}$, where $P_{SAT}$ is significantly below the $P_{BURST}$ pressures under investigation).

Solution results are presented in Figures 6 - 13 and these are discussed below.

**Initiating Pressurization/Discharge From the Agent's Saturation State; No $N_2$ in the Discharge Vessel at t = 0**

Simulations were carried out for experiments where the pressurization/discharge processes were initiated at the test agent's saturation state, i.e., at $P_{DV,1}$ = $P_{SAT}(T_{DV,1}$ = 294K) = $9.38x10^5$Pa (136psi), e.g., shortly after filling the evacuated vessel with the test agent. In such experiments there is no $N_2$ in the discharge vessel at t = 0, i.e., $M_{DV,N2,1}$ = 0. Results of the calculations are plotted in Figures 6 - 11.

The pressurization process. Figure 6 presents plots of $P_{DV}$ and $P_{HT}$ during vessel pressurization, 0 < t < $t_{BURST}$. Results are presented for the three orifice diameters, $D_O$ = 0.005m, 0.001m, and 0.0005m.

As seen in Figure 6, for the smallest orifice, $D_O$ = 0.0005m, the pressurization process, when $P_{DV,1} \leq P_{DV} < P_{BURST}$, takes 4.2s [for $P_{BURST}$ = $37.92x10^5$Pa (550psi)] to 5.8s [for $P_{BURST}$ = $44.82x10^5$Pa (650psi)]. For the intermediate-size orifice, $D_O$ = 0.001m, the pressurization process takes 1.0s (for $P_{BURST}$ = 550psi) to 1.4s (for $P_{BURST}$ = 650psi). For the largest orifice, $D_O$ = 0.005m, the entire process takes place within 0.1s.

$U_{JET}$ values corresponding to Figure 6 are presented in Figure 7. For the smallest orifice, $D_O$ = 0.0005m, $U_{JET}$ starts out at approximately 4m/s and drops to 2 - 3m/s at $t_{BURST}$, the time of diaphragm bursting. For $D_O$ = 0.001m, $U_{JET}$ starts out at approximately 8m/s and drops to approximately 4m/s at $t_{BURST}$. For $D_O$ = 0.005m, $U_{JET}$ starts out at approximately 40m/s and drops to as low as approximately 16m/s [for $P_{BURST}$ = $44.82x10^5$Pa (650psi)] at $t_{BURST}$.

Based on the above results it is concluded that during the pressurization process and relative to the criterion of Eq. (15): 1) use of the large orifice would lead to conditions which do not satisfy the criterion; 2) use of the intermediate size orifice would lead to results which are barely acceptable; and 3) use of the small orifice would lead to acceptable performance, provided that pressurization times are consistent with timing requirements of the photographic data acquisition system.

The discharge process. Figures 8 - 11 present plots of $U_{JET}$, dZ/dt, $Z/Z_1$, and $(M_{N2} - M_{N2,B})/M_{N2,B}$ during the discharge process. For the limiting burst pressures, $P_{BURST}$ = $37.92x10^5$Pa (550psi) and $44.82x10^5$Pa (650psi), results are presented for the small- and large-orifice designs.

Figure 8 presents results for $P_{BURST}$ = $37.92x10^5$Pa (550psi) and $D_O$ = 0.0005m. Once the discharge process is initiated, the liquid is seen to drop from its initial elevation ($Z/Z_1$ = 1) and to be removed entirely from the vessel ($Z/Z_1 \rightarrow 0$) in approximately 0.024s. Liquid discharge occurs at a relatively uniform rate with dZ/dt dropping from approximately 7.0 to 4.5 m/s during the emptying process. During discharge $U_{JET}$ first rises slightly (because of relatively rapid reductions of $P_{DV}$, slow reductions of $P_{HT}$, and resulting increases in cross-orifice pressure difference) from approximately 3 m/s, and then drops (because of the significantly increased length along the jet axis between the source of the jet, at the orifice, and the elevation at the gas/liquid interface - refer to Figures 1 and 2) to the final value of approximately 2m/s. As can be seen from the plot of $(M_{N2} - M_{N2,B})/M_{N2,B}$, during the entire emptying process the total mass addition of $N_2$ from the holding tank to the discharge vessel is less than one percent of the initial $N_2$ mass in the discharge vessel.

Figure 9 presents results for $P_{BURST}$ = 37.92x10$^5$Pa (550psi) and $D_O$ = 0.005m. Based on an approximate extrapolation from t - $t_{BURST}$ = 0.020s, once the discharge process is initiated the liquid is seen to drop from its initial elevation and to be removed entirely from the vessel in approximately 0.023s. Liquid discharge occurs at a relatively uniform rate with dZ/dt dropping from approximately 7.0 to 5.5m/s during the emptying process. During discharge $U_{JET}$ first rises slightly from approximately 30m/s, and then drops to the final value of approximately 20m/s. As can be seen from the plot of $(M_{N2} - M_{N2,B})/M_{N2,B}$, during the entire emptying process the total mass addition of $N_2$ from the holding tank to the discharge vessel is significant, approximately 45 percent of the initial $N_2$ mass in the discharge vessel.

Figure 10 presents results for $P_{BURST}$ = 44.82x10$^5$Pa (650psi) and $D_O$ = 0.0005m. Here the discharge is completed in 0.023s. Liquid discharge occurs at a relatively uniform rate with dZ/dt dropping from approximately 7.5 to 5.0m/s during the emptying process. During discharge $U_{JET}$ first rises from approximately 1 to 2m/s, and then drops back to the final value of approximately 1m/s. During the discharge the total mass addition of $N_2$ from the holding tank to the discharge vessel is less than one percent of the initial $N_2$ mass in the discharge vessel.

Figure 11 presents results for $P_{BURST}$ = 44.82x10$^5$Pa (650psi) and $D_O$ = 0.005m. From this it is seen that discharge occurs in approximately 0.021s. Liquid discharge occurs at a relatively uniform rate with dZ/dt dropping from approximately 7.5 to 5.5m/s during the emptying process. During discharge $U_{JET}$ first rises from approximately 17 to 25m/s, and then drops to the final value of approximately 20m/s. During the discharge the total mass addition of $N_2$ from the holding tank to the discharge vessel is approximately 40 percent of the initial $N_2$ mass in the discharge vessel.

Based on the above results it is concluded that during the discharge process and relative to the criteria of Eqs. (14) and (15): 1) use of the large orifice would lead to conditions which violate both of the criterion; 2) use of the small orifice would lead to acceptable performance.

**Initiating the Pressurization/Discharge Sequence From a $P_{DV,I}$ Slightly Below $P_{BURST}$**

Simulations were carried out for experiments initiated from a $P_{DV,I}$ which is slightly below $P_{BURST}$. Since the minimum possible $P_{BURST}$ is 37.92x10$^5$Pa (550psi), $P_{DV,I}$ is selected to be 34.47x10$^5$Pa (500psi).

The pressurization process. Figure 12 presents plots of $P_{DV}$ and $P_{HT}$ during vessel pressurization. Results are presented for the three orifice diameters, $D_O$ = 0.005m, 0.001m, and 0.0005m.

As seen in Figure 12, for the smallest orifice, $D_O$ = 0.0005m, and for the diaphragm burst pressures under consideration, the pressurization process, $P_{DV,I} \le P_{DV} < P_{BURST}$, takes 0.6s [$P_{BURST}$ = 37.92x10$^5$Pa (550psi)] to 1.9s [$P_{BURST}$ = 44.82x10$^5$Pa (650psi)]. For the intermediate-size orifice, $D_O$ = 0.001m, the pressurization process takes 0.1s ($P_{BURST}$ = 550psi) to 0.5s ($P_{BURST}$ = 650psi). For the largest orifice, $D_O$ = 0.005m, the entire pressurization process takes place in less than 0.02s.

$U_{JET}$ values corresponding to Figure 12 are presented in Figure 13. For the smallest orifice, $D_O$ = 0.0005m, $U_{JET}$ starts out at approximately 3.5m/s and drops to 2.0 - 2.5m/s at the time of diaphragm rupture. For $D_O$ = 0.001m, $U_{JET}$ starts out at approximately 7m/s and drops to approximately 4.5m/s at the time of diaphragm rupture. For $D_O$ = 0.005m, $U_{JET}$ starts out at approximately 33m/s and drops to as low as approximately 21m/s [for $P_{BURST}$ = 44.82x10$^5$Pa (650psi)] at the time of diaphragm rupture.

Based on the above results it is concluded that during the pressurization process and relative to the criterion of Eq. (15), the present results for $P_{DV,I}$ = 34.47x10$^5$Pa (500psi) are similar to the earlier results for $P_{DV,I}$ = $P_{SAT}$ = 9.38x10$^5$Pa (136psi).

The discharge process. In the present case where $P_{DV,I}$ = 34.47x10$^5$Pa (500psi), results for the discharge process are very similar to the earlier results where $P_{DV,I}$ = $P_{SAT}$ = 136psi and are qualitatively well represented by the plots of Figures 8 - 11 and the earlier discussion of these.

**Comparing the Discharges of a Small-Orifice Test Configuration and a Field-Deployed System**

The model equations were also used to simulate the discharge of a field-deployed vessel filled with $CHClF_2$ and pressurized with $N_2$. At the onset of discharge the temperature in the vessel was taken to be 294K and, corresponding to the above calculations, the pressure in the vessel was taken to be 41.37x10$^5$Pa (600psi) [i.e., a nominal $P_{BURST}$ = 41.37x10$^5$Pa (600psi),

where simulating tests would involve experiments where $37.92x10^5Pa \leq P_{BURST} \leq 44.82x10^5Pa$ (550psi $\leq P_{BURST} \leq$ 650psi)]. In Figures 14 and 15 calculated values of $P_{DV}$ and $Z/Z_1$ for the deployed system simulation are compared with the values of these variables obtained in the above test simulations with $D_O = 0.0005m$. [The $P_{DV,1} = 9.38x10^5Pa$ (136psi) results are presented in the figures since these compare somewhat less favorably with the field-deployed system results than do the $P_{DV,1} = 34.47x10^5Pa$ (500psi) results.]

As can be seen in the figures, simulated field-deployed system results and simulated test results compare favorably.

**Summary of Results of Simulations Involving the Relatively Low-Pressure Large-Volume Holding Tank**

The above described model simulations lead to the following summary result:

> A Figure 1-type test configuration with a $0.25x10^{-3}m^3$ holding tank and a 0.0005m, and possibly a 0.001m-diameter orifice will provide experimental discharges which can be expected to simulate accurately the discharge of field-deployed systems. Of the two orifice sizes the smaller orifice is preferable. Use of a 0.005m diameter orifice can not be expected to adequately simulate field-deployed system discharges under the conditions studied.

It is expected that this result can be extended to a wide range of test parameters and test agents.

## RELATIVELY HIGH-PRESSURE SMALL-VOLUME HOLDING TANK

This section will present results for the pressurization/discharge sequence using a relatively high-pressure small-volume holding tank. $V_{HT} = 2.5x10^{-5}m^3$ is chosen to be one tenth of the initial gas volume in the discharge vessel and $P_{HT,1} = 155.13x10^5Pa$ (2250psi) is chosen to be large enough to insure that the amount of $N_2$ stored in the holding tank will rupture the diaphragm even when $P_{BURST}$ is at its maximum value, $44.82x10^5Pa$ (650psi).

The objective of choosing this combination of parameters is to attain a pressurization/discharge sequence which is so rapid, well within the above-mentioned 1s time interval, as to guarantee, without any significant timing considerations, successful acquisition of high-speed photographic data of the discharge process. The feature of a relatively small initial volume and mass of $N_2$ in the holding tank is only consistent with test sequences with relatively high initial $P_{DV,1}$'s, values close to the minimum possible diaphragm burst pressure. Thus, the present test parameters would not be expected to be useful in initiating the pressurization/discharge process from an initial state where the vessel contained only pure test agent at its saturation pressure. Here, $P_{DV,1}$ is again chosen to be $34.47x10^5Pa$ (500psi), slightly below $37.92x10^5Pa$ (550psi), the minimum value for $P_{BURST}$.

Solution results are presented in Figures 16 - 24.

**Pressurization and Discharge for the Small Orifice, $D_O = 0.0005m$**

Simulation results for pressurization/discharge test using the small orifice design are presented in Figures 16 - 20.

For $P_{BURST} = 37.92x10^5Pa$ (550psi), plots of $P_{DV}$ and $P_{HT}$ are presented in Figures 16 and plots of $U_{JET}$, $dZ/dt$, $Z/Z_1$, and $(M_{N2} - M_{N2,B})/M_{N2,B}$ in Figure 17. Note that the latter variable is meaningful only during discharge when $t \geq t_{BURST}$. As can be seen in these figures, for this case $t_{BURST} = 0.173s$, i.e., this is the time it takes for $P_{DV}$ to rise from $P_{DV,1} = 34.47x10^5Pa$ (500psi) to the diaphragm rupture pressure. From Figure 17 it is seen that the liquid is nearly all discharged from the vessel (i.e., $Z/Z_1$ is approaching zero) at approximately $t = 0.2s$. From Figure 17 it is also seen that during discharge: the rate of liquid outflow is reduced to about half of its original value, with $dZ/dt$ being reduced from 7.0m/s to 4.5m/s; $U_{JET}$ is reduced from an initial pre-discharge value of approximately 4m/s to approximately 2m/s; and $(M_{N2} - M_{N2,B})/M_{N2,B}$ rises from 0 to approximately 0.02, i.e. at the end of the discharge the mass of $N_2$ in the vessel is increased from its value at $t_{BURST}$ by a factor of approximately 0.02. The latter two results indicate that the criteria of Eqs. (14) and (13) are both satisfied and, in this sense, as with the relatively large holding tank, the small orifice design can be expected to adequately reproduce field-deployed discharges.

For $P_{BURST} = 44.82x10^5Pa$ (650psi), plots of $P_{DV}$ and $P_{HT}$ are presented in Figures 18 and plots of $U_{JET}$ and $dZ/dt$ are presented in Figure 19. Plots of $U_{JET}$, $dZ/dt$, $Z/Z_1$, and $(M_{N2} - M_{N2,B})/M_{N2,B}$ for the times of the discharge process are highlighted in Figure 20. For this case $t_{BURST} = 0.94s$. From Figure 18 it is seen that the $P_{HT}$ has almost been reduced to $P_{DV}$ at the time that discharge is initiated. Indeed, if the $P_{HT,1}$ had been much less than $155.13x10^5Pa$ (2250psi), $P_{DV}$

would not have risen to $P_{BURST}$ and the discharge process would never have occurred! From Figure 19 it is seen that during the pressurization process $U_{JET}$ is reduces from approximately 4.0m/s to 1.5m/s. The liquid is nearly all discharged from the vessel at 0.962s. During discharge: dZ/dt is reduced from 7.5m/s to 5.0m/s; $U_{JET}$ rises to approximately 2.5m/s from its initial value of 1.5m/s and finally drops to approximately 2m/s; and $(M_{N2} - M_{N2,B})/M_{N2,B}$ rises from 0 to approximately 0.005. The criteria of Eqs (14) and (15) are again satisfied.

As noted, for both $P_{BURST} = 37.92x10^5$Pa (550psi) and $44.82x10^5$Pa (650psi) the above results indicate that both criteria of Eq. (14) and (15) are satisfied with the small-holding-tank/small-orifice design and that in this sense this design can be expected to adequately reproduce field-deployed discharges. However, for the following three reasons the large-holding-tank design is significantly more robust than the small-holding-tank design:

1. For a given maximum value for $P_{BURST}$, and discharge vessel volume, the minimum acceptable value for $P_{HT,1}$ [approximately $155.13x10^5$Pa (2250psi) for the present test parameters] is very sensitive to the original amount of liquid in the vessel. For example, in the present simulations the vessel was assumed to be one-half full; but if it were only one-quarter full, the minimum $P_{HT,1}$ that would lead to rupture of the $44.82x10^5$Pa (650psi) diaphragm would have been approximately $206.84x10^5$Pa (3000psi).

2. The small-volume-holding tank configuration does not allow for the option of initiating tests from relatively-low values of $P_{DV,1}$, e.g. immediately after filling the vessel with the test agent, when $P_{DV,1} = P_{SAT}$. To do so would once again require highly variable and unreasonably large values of $P_{HT,1}$.

3. The large-holding-tank design requires $P_{HT,1}$ values only slightly greater than the maximum $P_{BURST}$ value and it suffers from neither of the above shortcomings.

**Pressurization and Discharge for the Large Orifice, $D_O = 0.005$m**

Simulation results for pressurization/discharge test using the large-orifice design are presented in Figures 21 - 24.

For $P_{BURST} = 37.92x10^5$Pa (550psi), plots of $P_{DV}$ and $P_{HT}$ are presented in Figures 21 and plots of $U_{JET}$, dZ/dt, $Z/Z_1$, and $(M_{N2} - M_{N2,B})/M_{N2,B}$ in Figure 22. Note that the latter variable is meaningful only during discharge when $t \geq t_{BURST}$. As can be seen in these figures, for this case $t_{BURST} = 0.00173$s, i.e., this is the time it takes for $P_{DV}$ to rise from $P_{DV,1} = 34.47x10^5$Pa (500psi) to the diaphragm rupture pressure. From Figure 21 is seen that the $P_{HT}$ has almost been reduced to $P_{DV}$ at t = 0.015s, at which time approximately 40 percent of the original amount of liquid is still in the vessel, i.e. $Z/Z_1 = 0.4$ (Figure 22). Also, from Figure 22 it is seen that the liquid is nearly all discharged from the vessel (i.e., $Z/Z_1$ is approaching zero) at approximately t = 0.023s. From Figure 22 it is seen that during discharge: the rate of liquid outflow is reduced to about half of its original value, with dZ/dt going from 8m/s to 4m/s; $U_{JET}$ is always dropping, being reduced from an initially large pre-discharge value of approximately 40m/s to approximately 4m/s; and $(M_{N2} - M_{N2,B})/M_{N2,B}$ rises from 0 to 0.35, i.e. at the end of the discharge the mass of $N_2$ in the vessel is increased from its value at $t_{BURST}$ by a factor of approximately 0.35. The latter two results indicate that the criteria of Eqs. (14) and (15) are not satisfied and, as when used in conjunction with a relatively large holding tank, the large orifice design is not expected to adequately reproduce field-deployed discharges.

For $P_{BURST} = 44.82x10^5$Pa (650psi), plots of $P_{DV}$ and $P_{HT}$ are presented in Figures 23 and plots of $U_{JET}$, dZ/dt, $Z/Z_1$, and $(M_{N2} - M_{N2,B})/M_{N2,B}$ in Figure 24. The results are qualitatively similar to those discussed in the last paragraph for $P_{BURST} = 37.92x10^5$Pa (550psi). The quantitative differences can be easily determined from the figures. For this case $t_{BURST} = 0.0094$s. From Figure 23 is seen that the $P_{HT}$ has almost been reduced to $P_{DV}$ at the time that discharge is initiated. Indeed, if the $P_{HT,1}$ had been much less than $155.13x10^5$Pa (2250psi), $P_{DV}$ would not have risen to $P_{BURST}$ and the discharge process would never have occurred! The liquid is nearly all discharged from the vessel at 0.03s. During pressurization process $U_{JET}$ drops from approximately 40m/s to 15m/s. During discharge: dZ/dt is reduced from 7m/s to 5m/s; $U_{JET}$ is reduced from 15m/s to 3.5m/s; and $(M_{N2} - M_{N2,B})/M_{N2,B}$ rises from 0 to 0.1. Although the criterion of Eq. (14) is satisfied, that of Eq. (15) is not.

## SUMMARY AND CONCLUSIONS

A mathematical model and associated computer program were developed to simulate the discharge of fire extinguishment agents from $N_2$-pressurized vessels. The model is expected to have three applications. First, to establish an experimental

procedure which both 1) simulates de-pressurization of a field-deployed discharge vessel and 2) allows for acquisition of data, including high speed photography, to chracterize adequately the discharge process. Second, to evaluate the discharge characteristics of a wide range of alternative-agent/pressure-vessel configurations, thereby extending the slow and relatively costly experimental method of making such evaluations. Finally, to predict exit flow conditions to be used to solve the problem of agent dispersal outside of the discharge vessel. The model is based on the experimental configuration depicted in Figure 1, and the solution method is capable of treating arbitrary choices of geometric parameters, material properties, and initial conditions.

The model was used in example calculations which address the first of the applications, viz., the establishment of a robust experimental design and procedure that would 1) simulate the discharge of field-deployed fire extinguishment systems useable in US Air Force aircraft and 2) meet additional experimental constraints consistent with a program at NIST in support of the US Air Force fire safety issues.

In the example calculations, the fixed parameters which characterized the system were a half-liter discharge vessel with a circular exit nozzle/orifice of diameter 0.01905m half-filled with Freon 22 in the liquid phase at "room temperature," 294K.

The deployed system was assumed to be pressurized with $N_2$ to a total pressure of $41.37 \times 10^5$Pa (600psi), where the exit nozzle/orifice is closed with an explosive cap which is released "on demand." In the experimental system, the exit nozzle/orifice is capped with a disk which ruptures at an *a priori*-unknown pressure, between $37.92 \times 10^5$Pa (550psi) and $44.82 \times 10^5$Pa (650psi).

The experimental system, is brought to the rupture/burst pressure, $P_{BURST}$, from an initial pressure $P_{DV,1}$ by a process of pressurization by flow from the holding tank which is initially filled with $N_2$ at some pressure, $P_{HT,1}$, higher than $P_{BURST}$. The holding tank communicates with the discharge vessel through a circular orifice of diameter $D_O$.

The model was used to simulate the discharge of the deployed system and of the experimental system. Experimental parameters that were varied were $P_{DV,1}$ [$9.38 \times 10^5$Pa (136psi) or $34.47 \times 10^5$Pa (500psi)]; $P_{HT,1}$ and the volume of the holding tank [$51.71 \times 10^5$Pa (750psi) and $2.5 \times 10^{-3}$m$^3$, or $155.13 \times 10^5$Pa (2250psi) and $2.5 \times 10^{-5}$m$^3$]; and $D_O$ (0.005m, 0.001m, or 0.0005m).

Results of the simulations were presented in Figures 6 - 24.

Based on the model calculations it was determined that with $P_{DV,1} = 9.38 \times 10^5$Pa (136psi) or $34.47 \times 10^5$Pa (500psi) an experimental configuration/design using the relatively low-pressure [$51.71 \times 10^5$Pa (750psi)], large-volume ($2.5 \times 10^{-3}$m$^3$), holding tank and the smallest-diameter (0.0005m) orifice would accurately simulate the discharge of the field-deployed system. Furthermore, it is expected that such a design is robust in the sense that it would also simulate well the field-deployed system even when extended to a range of parameters and agent materials well beyond the scope of the present calculations.

Model calculations also indicated that an experimental design which uses the large-diameter orifice (0.005m) and/or the relatively-high pressure small-volume holding tank [$155.13 \times 10^5$Pa (2250psi) and $2.5 \times 10^{-5}$m$^3$] would often not provide accurate simulations of field-deployed discharges and would never be expected to be "robust."

Validation of the model requires experimental confirmation of model predictions.

## ACKNOWLEDGEMENT

The author acknowledges the support of the U.S. Air Force Wright Patterson Laboratory in carrying out this investigation.

## REFERENCES

[1] Shapiro, A.H., The Dynamics and Thermodynamics of Compressible Fluid Flow, Volume 1, Ronald Press, New York, 1953

[2] Model, M. and Reid, R.C., Thermodynamics and Its Applications, Prentice Hall, Englewood Cliffs, NJ, 1983.

[3] Kim-E, M.E. and Reid, R.C., The Rapid Depressurization of Hot, High Pressure Liquids or Supercritical Fluids, Chemical Engineering at Critical Fluid Conditions, Paulaitis, M.E. *et al*, Eds., Ann Arbor Science, pp. 81-100, 1981.

[4] Benjamin, M.W. and Miller, J.G., The Flow of Saturated Water Through Throttling Orifices, Trans. Am. Soc. Mech. Engrs., Vol. 63, pp. 419-429, 1941.
[5] Yang, J.C., private communication.
[6] Cooper, L.Y., Discharge of Fire Suppression Agents From a Pressurized Vessel: A Mathematical Model and Its Application to Experimental Design, NISTIR, National Institute of Standards and Technology, Gaithersburg MD, 1993.
[7] Abramowitz, G.N., The Theory of Turbulent Jets, MIT Press, Cambridge, MA, p. 82-84, 1963.
[8] Press, W.H. *et al*, Numerical Recipes - The Art of Scientific Computing, Cambridge University Press, 1986.
[9] Bracker, W. and Mossman, A.L., Matheson Unabridged Gas Data Book on Chlorodifluoromethane/$CHClF_2$ (Fluorocarbon-22), Matheson, Lyndhurst, NJ, 1974.
[10] Reid,R.C. *et al*, The Properties of Gases and Liquids, Appendix A, 3rd Edition, McGraw Hill, 1977.
[11] Perry, J.A., Critical Flow Through Sharp-Edged Orifices, Trans. American Soc. Mech. Eng., 71, pp. 757-764, 1949.

**NOMENCLATURE**

| | |
|---|---|
| $A_{DV}$ | cross-section area of discharge vessel |
| $A_N$, $A_O$ | area of discharge nozzle/orifice, orifice from holding tank |
| $C_{D,N}$, $C_{D,O}$ | flow coefficient of discharge nozzle/orifice, orifice from holding tank |
| $C_{P,AG}$, $C_{P,N2}$ | specific heat at constant pressure of agent gas, $N_2$ |
| $C_{V,AG}$, $C_{V,N2}$ | specific heat at constant volume of agent gas, $N_2$ |
| $D_{DV}$, $D_N$ | diameter of discharge vessel, its exit nozzle/orifice |
| $D_O$ | diameter of the orifice between discharge vessel and holding tank |
| $M_{DV,AG}$, $M_{DV,AL}$ | mass of gaseous, liquid agent in discharge vessel |
| $M_{DV,N2}$, $M_{HT,N2}$ | mass of $N_2$ in discharge vessel, holding tank |
| $M_{DV,N2,1}$, $M_{DV,AL,1}$, $M_{HT,N2,1}$ | $M_{DV,N2}$, $M_{DV,AL}$, $M_{HT,N2}$ at t = 0 |
| $M_{N2}$ | total mass of $N_2$ in discharge vessel and holding tank, see Eq. (3) |
| $M_{N2,B}$ | mass of $N_2$ in discharge vessel when the diaphram ruptures |
| P | pressure |
| $P_{AMB}$ | P of ambient environment |
| $P_{BURST}$ | P in discharge vessel when the diaphram ruptures |
| $P_{DV}$, $P_{HT}$ | P in discharge vessl, holding tank |
| $P_{DV,1}$, $P_{HT,1}$ | $P_{DV}$, $P_{HT}$ at t = 0 |
| $P_{SAT}$ | P when liquid agent is at saturation |
| $P_{SP}$ | P on agent spinoidal curve |
| $R_{AG}$, $R_{N2}$ | gas constants for gaseous agent, $N_2$ |
| T | temperature |
| $T_{AL}$ | T of liquid agent |
| $T_{DV}$, $T_{HT}$ | T of gaseous agent in discharge vessel, $N_2$ in holding tank |
| $T_{DV,1}$, $T_{HT,1}$ | $T_{DV}$, $T_{HT}$ at t = 0 |
| t | time from begining of experiment or from onset of discharge of field-deployed system |
| $t_{BURST}$ | t when diaphram ruptures |
| $t_D$ | t at completion of liquid discharge or when $P_{DV}$ reaches $P_{SAT}$ during discharge |
| $U_{JET}$, $U_O$ | axial velocity of orifice jet upstream of gas/liquid interface |
| $V_{DV}$, $V_{HT}$ | volume of discharge vessel, holding tank |
| $x_1$, $x_2$, $x_3$ | variables of dimensionless initial value problem, Eq. (9) |
| Z | elevation of gas/liquid interface above bottom of discharge vessel |
| $Z_1$ | Z at t = 0 |
| $Z_{DV}$ | length of discharge vessel |
| $Z_{JET}$ | $Z_{DV}$ - Z |
| $\gamma$, $\gamma_{AG}$ | ratio of specific heats for $N_2$, gaseous agent |
| $\rho_{AL}$ | density of liquid agent |
| $\rho_{SAT}$ | density of saturated liquid agent |
| $\lambda_i$ | dimensionsless parameters, i = 1 to 4, Eqs. (10) |
| $\sigma_i$ | functions of $x_i$ and parameters, i = 1, 2, 3, Eqs. (11) |
| $\tau$ | dimensionless t, Eqs. (9) |

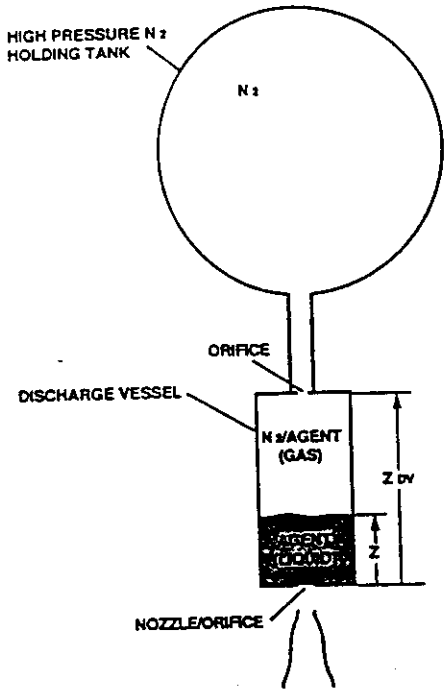


Figure 1. The experimental arrangement.

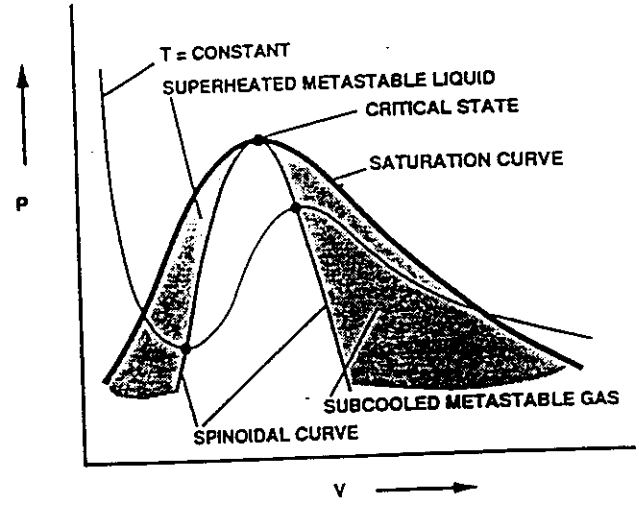


Figure 2. P-V diagram for a generic material; the spinoidal curve and regions of metastable liquid and vapor.

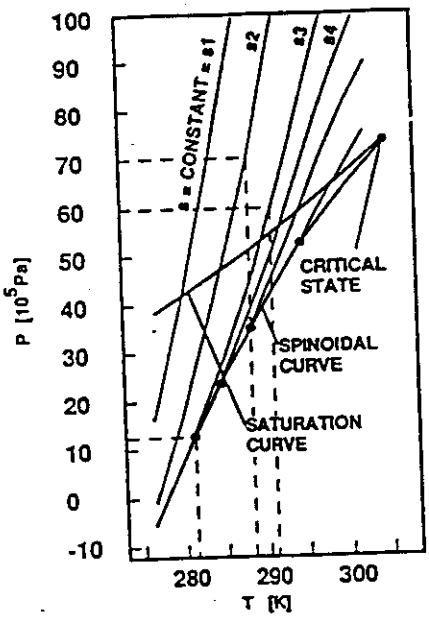


Figure 3. P-T diagram for metastable liquid $CO_2$ [3].

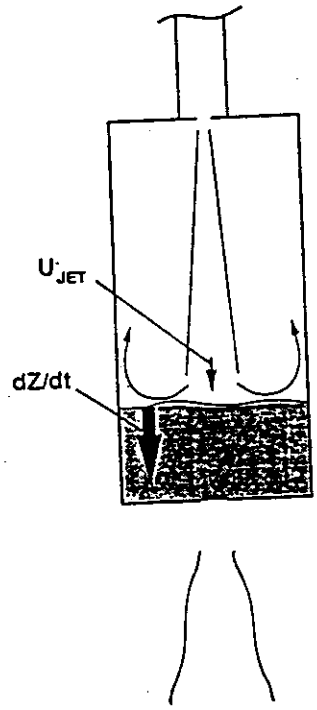


Figure 4. Sketch of the orifice-driven $N_2$ jet flow in the discharge vessel.

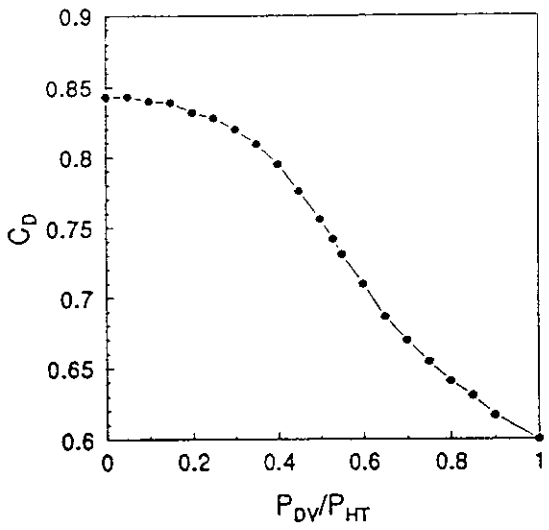


Figure 5. Discharge coefficient, $C_{D,O}$, for compressible flow through a sharp-edged orifice as a function of cross-orifice pressure ratio, $P_{DV}/P_{HT}$ [11].

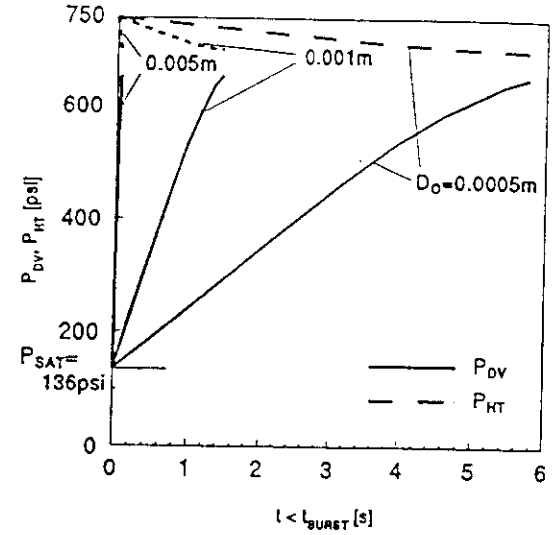


Figure 6. Plots of $P_{DV}$ and $P_{HT}$ for $0 \leq t \leq t_{BURST}$ and $D_O$ = 0.005m, 0.001m, and 0.0005m; where $V_{HT}$ = $2.5x10^{-3}m^3$, $T_{DV,1} = T_{HT,1}$ = 294K, $P_{DV,1} = P_{SAT}$ = $9.38x10^5$Pa (136psi), $P_{HT,1}$ = $51.71x10^5$Pa (750psi), $P_{BURST} \leq 44.82x10^5$Pa (650psi).

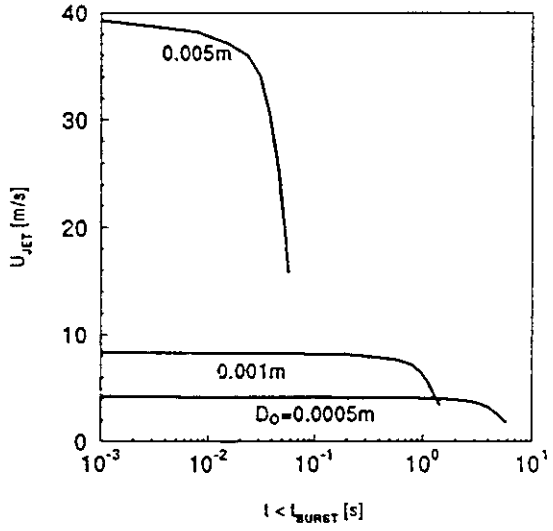


Figure 7. Plots of $U_{JET}$ for $0 \leq t \leq t_{BURST}$ and $D_O$ = 0.005m, 0.001m, and 0.0005m; where $V_{HT}$ = $2.5x10^{-3}m^3$, $T_{DV,1} = T_{HT,1}$ = 294K, $P_{DV,1} = P_{SAT}$ = $9.38x10^5$Pa (136psi), $P_{HT,1}$ = $51.71x10^5$Pa (750psi), $P_{BURST} \leq$ $44.82x10^5$Pa (650psi).

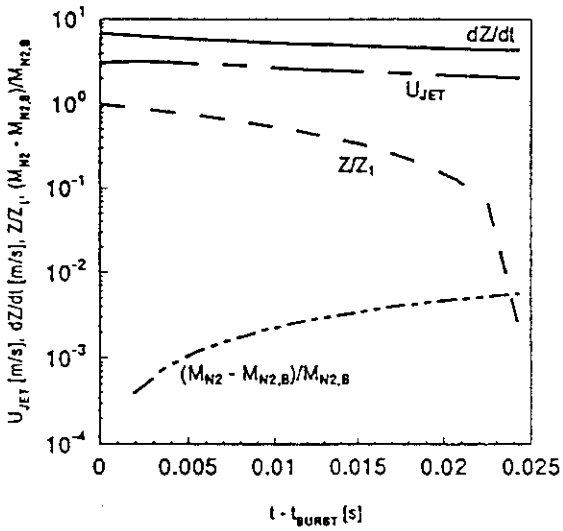


Figure 8. Plots of $U_{JET}$, dZ/dt, $Z/Z_1$, and $(M_{N2} - M_{N2,B})/M_{N2,B}$ for $t \geq t_{BURST}$; where $V_{HT}$ = $2.5x10^{-3}m^3$, $T_{DV,1} = T_{HT,1}$ = 294K, $P_{DV,1} = P_{SAT}$ = $9.38x10^5$Pa (136psi), $P_{HT,1}$ = $51.71x10^5$Pa (750psi), $P_{BURST}$ = $37.92x10^5$Pa (550psi) and $D_O$ = 0.0005m.

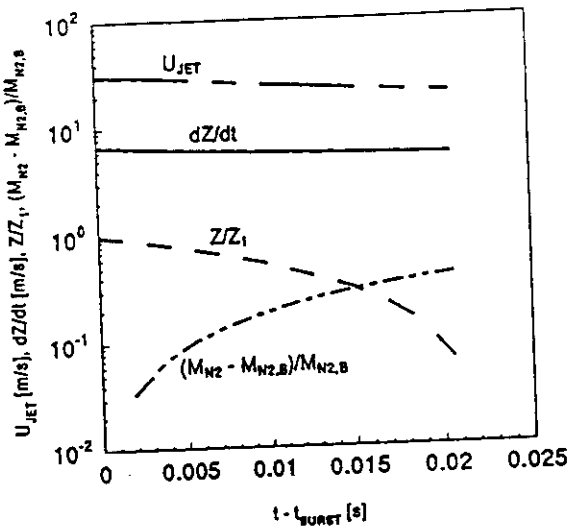


Figure 9. Plots of $U_{JET}$, dZ/dt, $Z/Z_1$, and $(M_{N2} - M_{N2,B})/M_{N2,B}$ for $t \geq t_{BURST}$; where $V_{HT} = 2.5x10^{-3}m^3$, $T_{DV,1} = T_{HT,1} = 294K$, $P_{DV,1} = P_{SAT} = 9.38x10^5Pa$ (136psi), $P_{HT,1} = 51.71x10^5Pa$ (750psi), $P_{BURST} = 37.92x10^5Pa$ (550psi) and $D_O = 0.005m$.

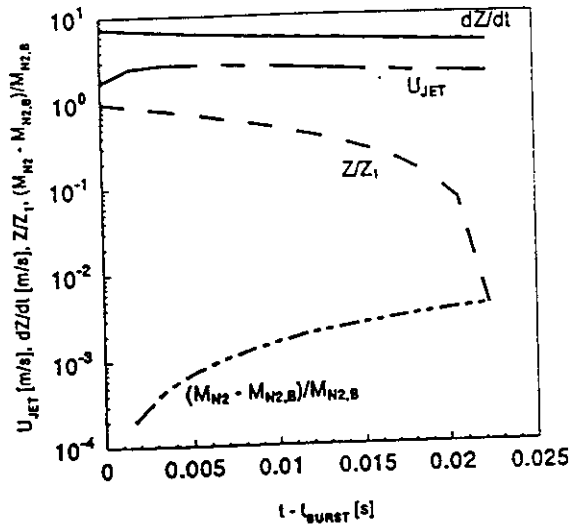


Figure 10. Plots of $U_{JET}$, dZ/dt, $Z/Z_1$, and $(M_{N2} - M_{N2,B})/M_{N2,B}$ for $t \geq t_{BURST}$; where $V_{HT} = 2.5x10^{-3}m^3$, $T_{DV,1} = T_{HT,1} = 294K$, $P_{DV,1} = P_{SAT} = 9.38x10^5Pa$ (136psi), $P_{HT,1} = 51.71x10^5Pa$ (750psi), $P_{BURST} = 44.82x10^5Pa$ (650psi) and $D_O = 0.0005m$.

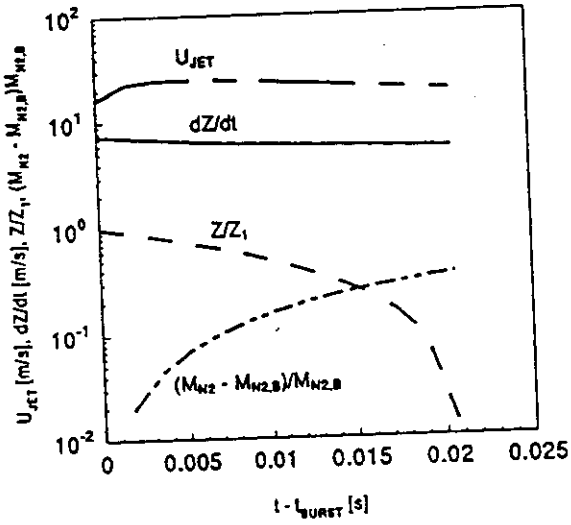


Figure 11. Plots of $U_{JET}$, dZ/dt, $Z/Z_1$, and $(M_{N2} - M_{N2,B})/M_{N2,B}$ for $t \geq t_{BURST}$; where $V_{HT} = 2.5x10^{-3}m^3$, $T_{DV,1} = T_{HT,1} = 294K$, $P_{DV,1} = P_{SAT} = 9.38x10^5Pa$ (136psi), $P_{HT,1} = 51.71x10^5Pa$ (750psi), $P_{BURST} = 44.82x10^5Pa$ (650psi) and $D_O = 0.005m$.

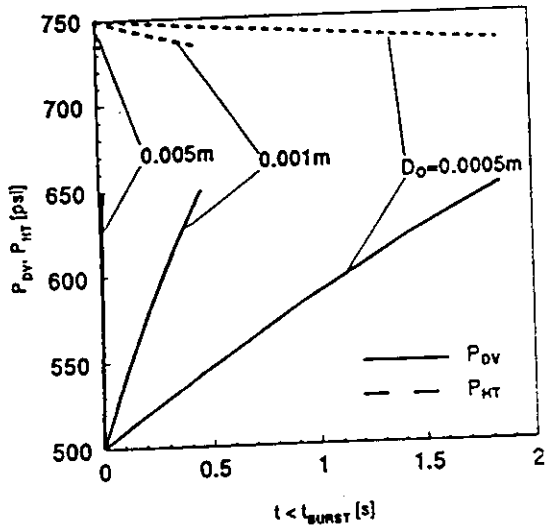


Figure 12. Plots of $P_{DV}$ and $P_{HT}$ for $0 \leq t \leq t_{BURST}$ and $D_O = 0.005m$, 0.001m, and 0.0005m; where $V_{HT} = 2.5x10^{-3}m^3$, $T_{DV,1} = T_{HT,1} = 294K$, $P_{DV,1} = 34.47x10^5Pa$ (500psi), $P_{HT,1} = 51.71x10^5Pa$ (750psi), $P_{BURST} \leq 44.82x10^5Pa$ (650psi).

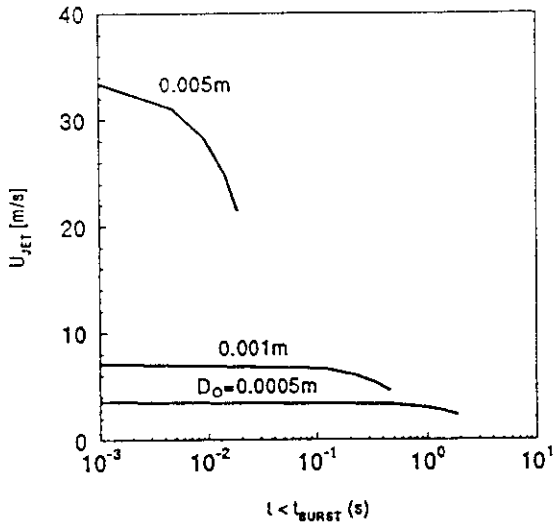


Figure 13. Plots of $U_{JET}$ for $0 \leq t \leq t_{BURST}$ and $D_O$ = 0.005m, 0.001m, and 0.0005m.; where $V_{HT} = 2.5x10^{-3}m^3$, $T_{DV,1} = T_{HT,1} = 294K$, $P_{DV,1} = 34.47x10^5Pa$ (500psi), $P_{HT,1} = 51.71x10^5Pa$ (750psi), $P_{BURST} \leq 44.82x10^5Pa$ (650psi).

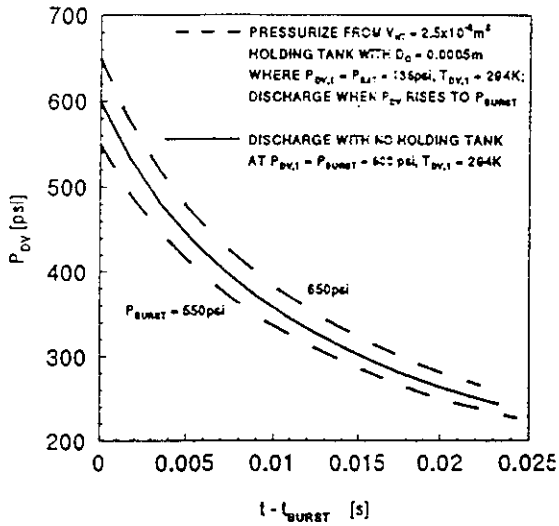


Figure 14. Plots of $P_{DV}$ during discharge of: 1) field-deployed vessel at $P_{BURST} = 41.37x10^5Pa$ (600psi) and test configuration vessel [$V_{HT} = 2.5x10^{-3}m^3$, $D_O$ = 0.0005m, $P_{DV,1} = P_{SAT}(294K) = 9.38x10^5Pa$ (136psi)] at 2) $P_{BURST} = 37.92x10^5Pa$ (550psi) and 3) $44.82x10^5Pa$ (650psi).

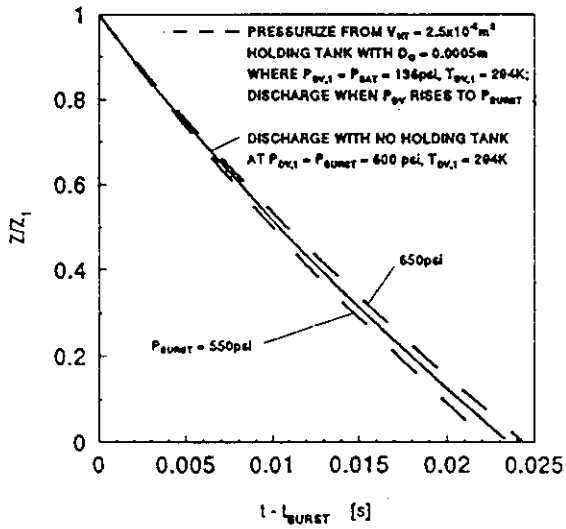


Figure 15. Plots of $Z/Z_1$ during discharge of: 1) field-deployed vessel at $P_{BURST} = 41.37x10^5Pa$ (600psi) and test configuration vessel [$V_{HT} = 2.510^{-3}m^3$, $D_O$ = 0.0005m, $P_{DV,1} = P_{SAT}(294K) = 9.38x10^5Pa$ (136psi)] at 2) $P_{BURST} = 37.92x10^5Pa$ (550psi) and 3) $44.82x10^5Pa$ (650psi).

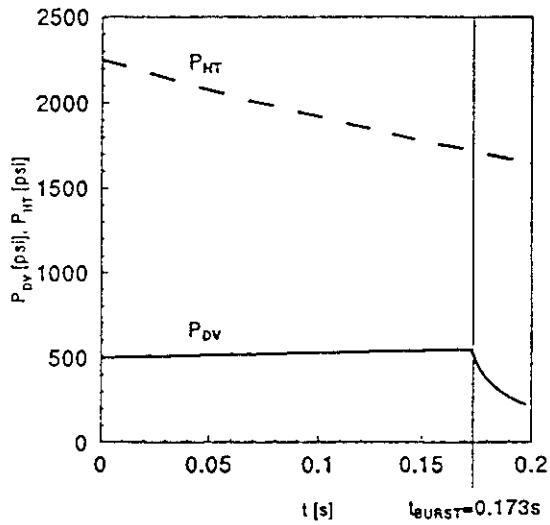


Figure 16. Plots of $P_{DV}$ and $P_{HT}$ for $t \geq 0$ and $D_O$ = 0.0005m; where $V_{HT} = 2.510^{-5}m^3$, $T_{DV,1} = T_{HT,1} = 294K$, $P_{DV,1} = 34.47x10^5Pa$ (500psi), $P_{HT,1} = 155.13x10^5Pa$ (2250psi), $P_{BURST} = 37.92x10^5Pa$ (550psi).

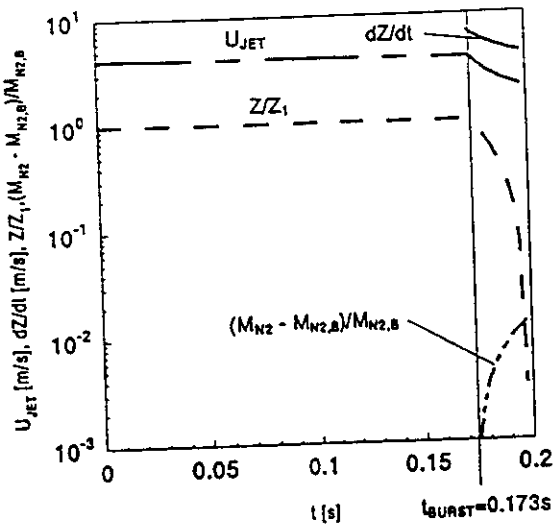


Figure 17. Plots of $U_{JET}$, dZ/dt, and Z/Z1, for $t \geq 0$ and dZ/dt, $Z/Z_1$, and of $(M_{N2} - M_{N2,B})/M_{N2,B}$ for $t \geq t_{BURST}$; where $V_{HT} = 2.5x10^{-5}m^3$, $D_O = 0.0005m$, $T_{DV,1} = T_{HT,1} = 294K$, $P_{DV,1} = 34.47x10^5Pa$ (500psi), $P_{HT,1} = 155.13x10^5Pa$ (2250psi), and $P_{BURST} = 37.92x10^5Pa$ (550psi).

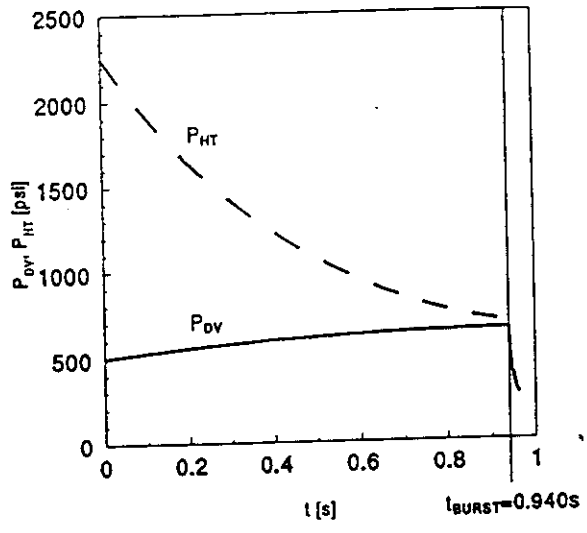


Figure 18. Plots of $P_{DV}$ and $P_{HT}$ for $t \geq 0$ and $D_O = 0.0005m$; where $V_{HT} = 2.5x10^{-5}m^3$, $T_{DV,1} = T_{HT,1} = 294K$, $P_{DV,1} = 34.47x10^5Pa$ (500psi), $P_{HT,1} = 155.13x10Pa$ (2250psi), $P_{BURST} = 44.82x10^5Pa$ (650psi).

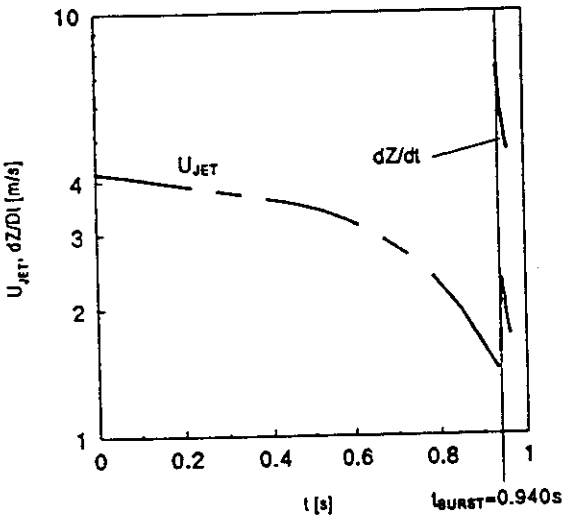


Figure 19. Plots of $U_{JET}$ and dZ/dt for $t \geq 0$ and $D_O = 0.0005m$; where $V_{HT} = 2.5x10^{-5}m^3$, $T_{DV,1} = T_{HT,1} = 294K$, $P_{DV,1} = 34.47x10^5Pa$ (500psi), $P_{HT,1} = 155.13X10^5Pa$ (2250psi), $P_{BURST} = 44.82x10^5Pa$ (650psi).

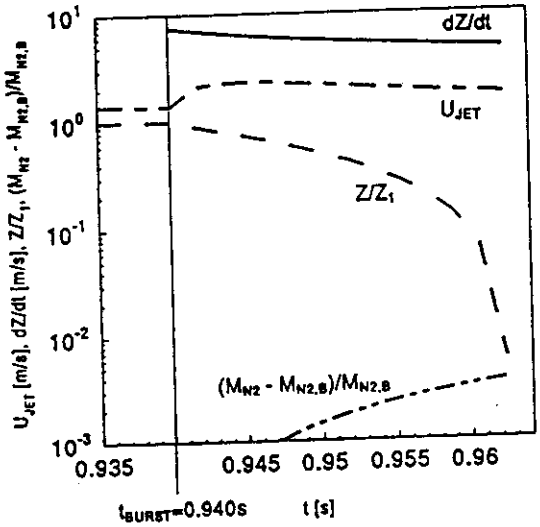


Figure 20. Plots of $U_{JET}$, dZ/dt, $Z/Z_1$, and $(M_{N2} - M_{N2,B})/M_{N2,B}$ for $t \geq t_{BURST}$ and $D_O = 0.0005m$; where $V_{HT} = 2.5x10^{-5}m^3$, $T_{DV,1} = T_{HT,1} = 294K$, $P_{DV,1} = 34.47x10^5Pa$ (500psi), $P_{HT,1} = 155.13x10^5Pa$ (2250psi), and $P_{BURST} = 44.82x10^5Pa$ (650psi).

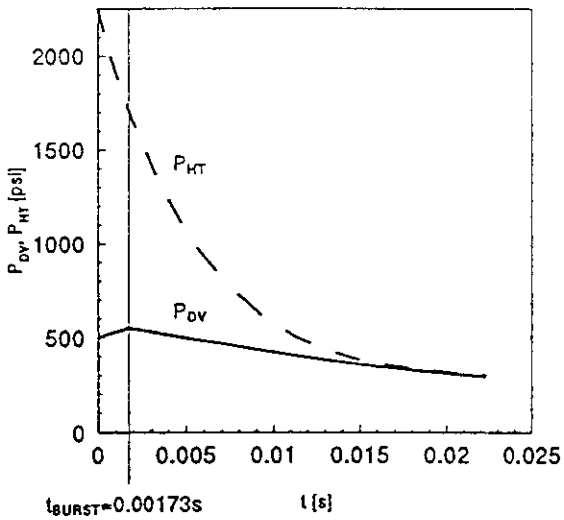


Figure 21. Plots of $P_{DV}$ and $P_{HT}$ for $t \geq 0$ and $D_O$ = 0.005m; where $V_{HT}$ = 2.5x10$^{-5}$m$^3$, $T_{DV,1} = T_{HT,1}$ = 294K, $P_{DV,1}$ = 34.47x10$^5$Pa (500psi), $P_{HT,1}$ = 155.13x10$^5$Pa (2250psi), $P_{BURST}$ = 37.92x10$^5$Pa (550psi).

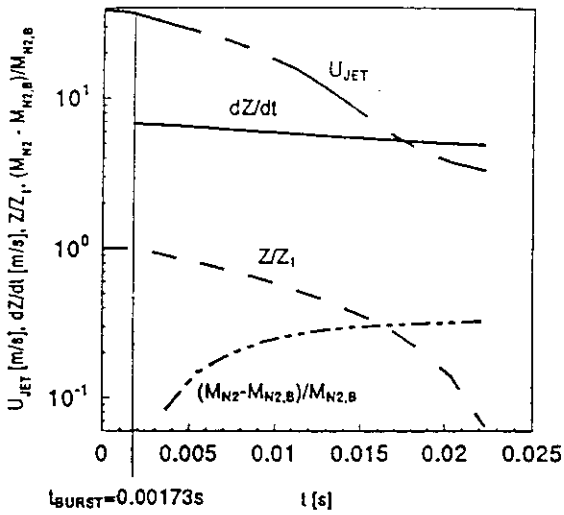


Figure 22. Plots of $U_{JET}$, dZ/dt, and Z/Z1, for $t \geq 0$ and dZ/dt, Z/Z$_1$, and of $(M_{N2} - M_{N2,B})/ M_{N2,B}$ for $t \geq t_{BURST}$; where $V_{HT}$ = 2.5x10$^{-5}$m$^3$, $D_O$ = 0.005m, $T_{DV,1} = T_{HT,1}$ = 294K, $P_{DV,1}$ = 34.47x10$^5$Pa (500psi), $P_{HT,1}$ = 155.13x10$^5$Pa (2250psi), and $P_{BURST}$ = 37.92x10$^5$Pa (550psi).

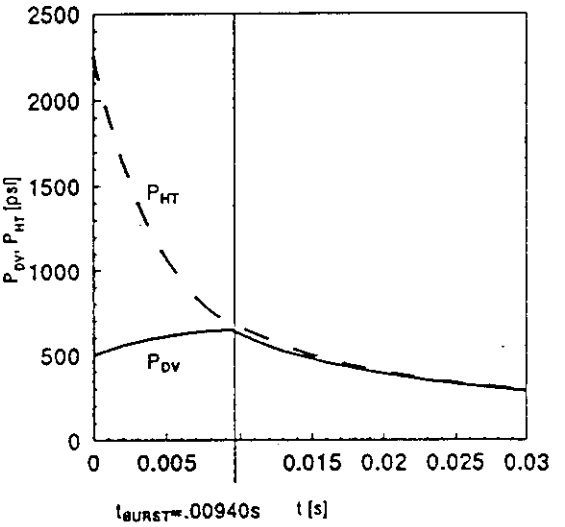


Figure 23. Plots of $P_{DV}$ and $P_{HT}$ for $t \geq 0$ and $D_O$ = 0.005m; where $V_{HT}$ = 2.5x10$^{-5}$m$^3$, $T_{DV,1} = T_{HT,1}$ = 294K, $P_{DV,1}$ = 34.47x10$^5$Pa (500psi), $P_{HT,1}$ = 155.13x10$^5$Pa (2250psi), $P_{BURST}$ = 44.82x10$^5$Pa (650psi).

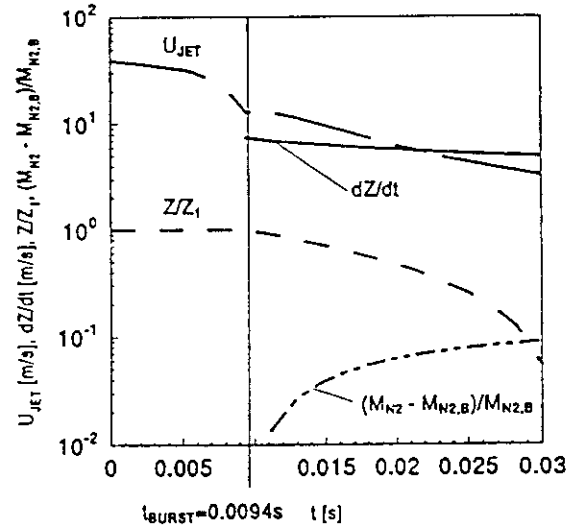


Figure 24. Plots of $U_{JET}$, dZ/dt, and Z/Z1, for $t \geq 0$ and dZ/dt, Z/Z$_1$, and of $(M_{N2} - M_{N2,B})/ M_{N2,B}$ for $t \geq t_{BURST}$; where $V_{HT}$ = 2.5x10$^{-5}$m$^3$, $D_O$ = 0.005m, $T_{DV,1} = T_{HT,1}$ = 294K, $P_{DV,1}$ = 34.47x10$^5$Pa (500psi), $P_{HT,1}$ = 155.13x10$^5$Pa (2250psi), and $P_{BURST}$ = 44.82x10$^5$Pa (650psi).